Geometries and Stabilities of Re-Doped Si_n ($n = 1-12$) Clusters: A Density Functional Investigation

Ju-Guang Han,*,†,‡ Zhao-Yu Ren,‡ and Ben-Zuo Lu§

National Synchrotron Radiation Laboratory and Department of Astronomy and Applied Physics, University of Science and Technology of China, Hefei 230026, People's Republic of China, and Institute of Photonics & Photon-Technology, Northwestern University, Xi'an 710068, People's Republic of China

Received: August 21, 2003; In Final Form: April 15, 2004

The possible $ReSi_n$ ($n = 1-12$) clusters are investigated systematically at the UB3LYP level employing LanL2DZ basis sets for a sequence of different spin states. The total energies and equilibrium geometries, as well as natural populations and natural electron configurations, are calculated. The emphasis on the stabilities and fragmentation energies as well as on electronic properties is presented and discussed. Theoretical results on natural populations reveal that the natural populations of 5d and 6s orbitals of the Re atom in $ReSi_n$ ($n = 1-12$) clusters are associated with the number of silicon atoms and spin of this species considered, that the natural population of the Re atom in the most stable $ReSi_n$ ($n = 1-12$) clusters is recorded as negative, and that the charges in the most stable $ReSi_n$ ($n = 1-12$) transfer from Si atoms and 6s orbitals of the Re atom to 5d orbitals of the Re atom. Therefore, the Re atom, which acts as an acceptor, plays an important role in the stability of $ReSi_n$ ($n = 1-12$) clusters. Furthermore, the charge-transfer of $ReSi_n$ ($n = 1-12$) depends on the spin of the species considered. Theoretical results of equilibrium geometries on $ReSi_n$ ($n = 1-12$) clusters show that the Re atom of the most stable $ReSi_n$ ($n = 1-7$) occupies a surface site and absorbs on the surface site of the Si cluster; however, the Re atom of the most stable $ReSi_n$ ($n = 8-12$) clusters is trapped in the center site of the Si cluster and directly interacts with all atoms simultaneously with nonequivalent bond lengths; this observation of transition metal (TM) behavior in TM−silicon clusters being favorable to the center site of the silicon frame when $n > 7$ is in good agreement with experimental measurement on $TbSi_x^-$ ($x = 6-16$) clusters. Growth patterns of $ReSi_n$ ($n = 9-12$) clusters are discussed showing the sandwichlike structure as the favorable structure. Relative stability is discussed upon removing one silicon atom, showing that $ReSi_2$ and the sandwichlike $ReSi_{12}$, $ReSi_{11}$, and $ReSi_9$ clusters have enhanced stability which is regarded as the abundance of the mass spectrometric observation on $ReSi_n^+$ ($n = 1-11$). These theoretical results are consistent with the atomic averaged binding energies also. Comparisons of $ReSi_n$ ($n = 1-12$) with available theoretical results of MSi_n ($n = 1-6$, M = Cr, Mo, W, Ir) cluster series and experimental measurements are made.

1. Introduction

The transition metal silicon clusters or cages have attracted attention, both theoretically and experimentally,[1−16] because the transition metal (TM) doped silicon cluster is a semiconducting cluster of great importance for applications in microelectronic technology and material science. There is currently great interest in utilizing small clusters as constituent elements to build up well-controlled nanostructures, at the surface or in the bulk of the material. This consideration provides strong motivation for the study of mixed TM−silicon clusters. In particular, the clusters are very stable and can be used as a tunable building block for cluster-assemble material. Furthermore, the charge-transfer, magnetism, superconductivity, and other properties of TM-doped silicon clusters are different from those of silicon clusters and bulk systems. Recently, considerable computational investigations were performed theoretically and aimed to invest in a computational search for fullerene-like silicon clusters stabilized by transition metal atoms. In addition, the theoretical investigations on TM−silicon clusters or fullerene-like TM−silicon structures provide the basis and information for future theoretical studies of TM−silicon nanotubes.

Beck and Hiura[3,11] have reported the experimental investigations of small mixed TM−silicon clusters (MSi_n; M = Cr, Mo, W, Ir, Re, Hf, Ta; $n < 19$) by mass spectrometry. Mixed transitional metal silicides have been produced by time-of-flight mass spectroscopy,[17] and the electronic states of CuSi, AgSi, and AuSi dimers were predicted by measuring their laser absorption spectra as well as by theoretical calculation using the CASPT2 method.[18] In addition, the VSi and NbSi dimers have been investigated by matrix-isolated ESP spectroscopy,[19] and their bond energies are reported experimentally.[20−22] The experimental investigation on iridium silicides by mass analysis, which includes the first gas-phase spectra for iridium silicides as well as the first direct evidence for the existence of polyatomic iridium silicides, is reported. The results of the iridium silicides ($IrSi_n$ and $IrSi_nH_{2n}$) provide insight into the information mechanism and properties of these species.[3]

* To whom correspondence should be addressed. Present address: Department of Chemistry & Biochemistry, Texas Tech University, Lubbock, TX 79409-1061. E-mail: jghan@ustc.edu.cn.

† National Synchrotron Radiation Laboratory, University of Science and Technology of China.

‡ Institute of Photonics & Photon-Technology, Northwestern University.

§ Department of Astronomy and Applied Physics, University of Science and Technology of China.

10.1021/jp031006o CCC: $27.50
Published on Web 05/15/2004

Experimental results[3] indicate that the relative abundance of Si_2-Ir is the largest of the $IrSi_n$ ($n = 1-6$) clusters, which is in good agreement with theoretical calculations;[9] furthermore, theoretical results indicate that the hydrogen atom in the $IrSi_nH_{2n}$ system influences the charge-transfer. In addition, some investigations on WSi_{12},[6] $ZrSi_{20}$ cages,[23] and cagelike MSi_{15} (M = Cr, Mo and W)[2] and $ReSi_x$ ($x = 16$, 20, 24, 28, 30, 32, 36, 40, 44, 60) clusters have been undertaken; moreover, the charge-transfer mechanisms and the equilibrium geometries of neutral MSi_n (M = Cr, Mo, W, Ir, Ni; $n = 1-6$) and MSi_m (M = Fe, Ru, Ag, Ta, Cu; $m = 1-12$)[1-2,4-6,8,9,24] clusters have been performed by use of the Gaussian 98 program[25] and ADF code.

Recently, experimental results on $ReSi_n^+$ ($n = 1-11$) and $ReSi_nH_m$ clusters, which provide the micromechanisms and properties of these species, were reported.[3] To achieve a detailed and systematic understanding of the clusters, it is important to investigate the evolution and properties of clusters with respect to the size of the system. The present work intends to serve these purposes, as it contains a comparison between various small $ReSi_n$ species, thereby containing a series of computational studies on small Si_nRe units that was recently started with an analysis of Si_nM (M = Cr, Mo, W, Ag, Ir; $n = 1-6$) clusters.[2,4,6,8,9] We try to examine if the localization of the Re atom upon/into silicon clusters changes the major rearrangement of the geometry framework of silicon clusters (or cages) as well as to reveal the striking change in properties due to the insertion of the various metals. We will concentrate on growth patterns in TM−silicon clusters.

The equilibrium geometries, stabilities, and electronic properties of Si_nRe ($n = 1-12$) clusters have not been determined theoretically, and surely, there is no systematic and theoretical investigation within the same approach. The main objective of this study, therefore, is to provide theoretical insight into values for the equilibrium geometries and stabilities as well as charge-transfer mechanisms of the rhenium silicides and to characterize the chemical bonding of $ReSi_n$ ($n = 1-12$) clusters. To give a reasonable and reliable explanation of the charge-transfer phenomenon and to compare available experimental results with theoretical data as well as to reveal the electronic properties of $ReSi_n$ ($n = 1-12$) clusters, computational investigations of total energies and equilibrium geometries as well as relative stabilities, along with the theoretical values of natural populations and natural electron configurations, are carried out by the density functional method in this paper.

2. Computational Details

In the present calculations, the DFT method is the UB3LYP[26] exchange-correlation potential using effective core potential (ECP) LanL2DZ basis sets.[27] The UB3LYP method consists of Becke's exchange functional[28] and the nonlocal LYP (Lee, Yang, and Parr) correlation correction functional. Theoretical predictions at the UB3LYP/LanL2DZ level are in good agreement with experimental observations. The application of ECP provides a considerable way to reduce difficulties in calculations of species containing heavy atoms, which are caused by a large number of two-electron integrals. The LanL2DZ basis sets become widely used in chemistry, particularly in the investigation of compounds or clusters containing heavy elements.[6,8] The standard LanL2DZ basis sets of ECP theory is consistent within the first, second, and third row TM containing systems. Furthermore, the LanL2DZ basis sets, which include the scalar relativistic effects, do not degrade when going from second to third row TM containing compounds.[4,6,8,9] On the other hand, it has been demonstrated that the LanL2DZ basis sets are capable of providing results of very satisfactory and reasonable quality for the geometries, stabilities, and spectroscopic properties of the TM compounds or clusters[6,8,9] with deviations of typically 1−6%. The detailed discussion of ECP is reported in refs 5, 8, and 9. For Cr_2, a bond length of 1.61 Å is found,[8] which is in good agreement with the experimental result (1.68 Å).

All theoretical computations are performed with the Gaussian 98[25] program package. Geometries are optimized at the UB3LYP[26-28] level employing LanL2DZ (Stuttgart/Dresden effective core potential) basis sets.[27,28] A systematic investigation of $ReSi_n$ ($n = 1-12$) clusters at the UB3LYP level employing LanL2DZ basis sets will give a general and reasonable conclusion. Comparison with theoretical calculations on Si_n and MSi_n (M = Cr, Mo, W, Ir) clusters[5,6,8,9,14] reveals that this method provides a reliable and reasonable result.[5,6] The Re_2 dimer is calculated, and theoretical results show that Re_2 with quintet spin configuration is the most stable structure, and that the Re−Re bond length is 2.136 Å. For each stationary point of the cluster, the stability is reassured by the harmonic vibrational frequencies. The spin contamination for TM−silicon clusters is non-negligible, and it is discussed in a previous paper in detail;[6] therefore, the discussion will not be presented in this paper. In addition, as the number of isomers increases rapidly with cluster size, it is very difficult to determine the global minimum simply according to the calculated energies of the isomers without reference to experimental or previous theoretical information. Fortunately, previous theoretical results on MSi_n (M = Ir, W, Cu, Mo) and experimental results on $ReSi_n^+$ ($n = 1-11$) are provided.[1-6,8-10]

3. Results and Discussions

3.1. Geometry and Stability. *ReSi.* The equilibrium geometry of the ReSi cluster with $C_{\infty v}$ symmetry taking into account the electron spin configurations of $S = 1/2$, 3/2, and 5/2 is optimized at the UB3LYP/LanL2DZ level (Figure 1). The Re−Si bond length of the ReSi cluster is of 2.203, 2.233, and 2.242 Å, respectively. Re−Si bond length is elongated as the spin configuration goes from $S = 1/2$, to $S = 3/2$, to $S = 5/2$ monotonically. The detailed mechanism of the TM−Si bond length varying with spin electron configurations is discussed in a previous paper with the aid of spin density.[6] Furthermore, the Re−Si bond length in the most stable ReSi is nearly the same as W−Si bond length of the most stable WSi cluster.[6] However, the total energies of the ReSi cluster with spin $S = 1/2$, 3/2, and 5/2 are −82.7757, −82.8323, and −82.7549 hartrees, respectively. Obviously, the quartet spin configuration is more stable than doublet spin configuration and sextet spin configuration by the energy differences of 1.542 and 2.106 eV, respectively. Therefore, the ReSi cluster with spin $S = 3/2$ is the most stable structure, which is selected as the ground state, and the corresponding electron state is labeled as having $^4\pi$ character. The spin configuration of the most stable ReSi cluster is similar to those of the WSi and MoSi clusters;[4,6] however, it is different from that of the IrSi cluster.[9]

$ReSi_2$. Guided by the previous theoretical results of $IrSi_2$ clusters,[9] the possible geometries of $ReSi_2$ clusters maintaining $D_{\infty h}$, C_s, C_{2v}, and $C_{\infty v}$ point-group symmetries (Figure 1) with the spin configurations considered are optimized. Equilibrium geometries and total energies are tabulated at Table 1. According to theoretical results of Table 1, we find that the linear $C_{\infty v}$ isomer is more stable than the linear $D_{\infty h}$ isomer with the same spin configuration. The remarkable Re−Si bond lengths of the linear $C_{\infty v}$ $ReSi_2$ clusters with spin $S = 1/2$, 3/2, and 5/2 are

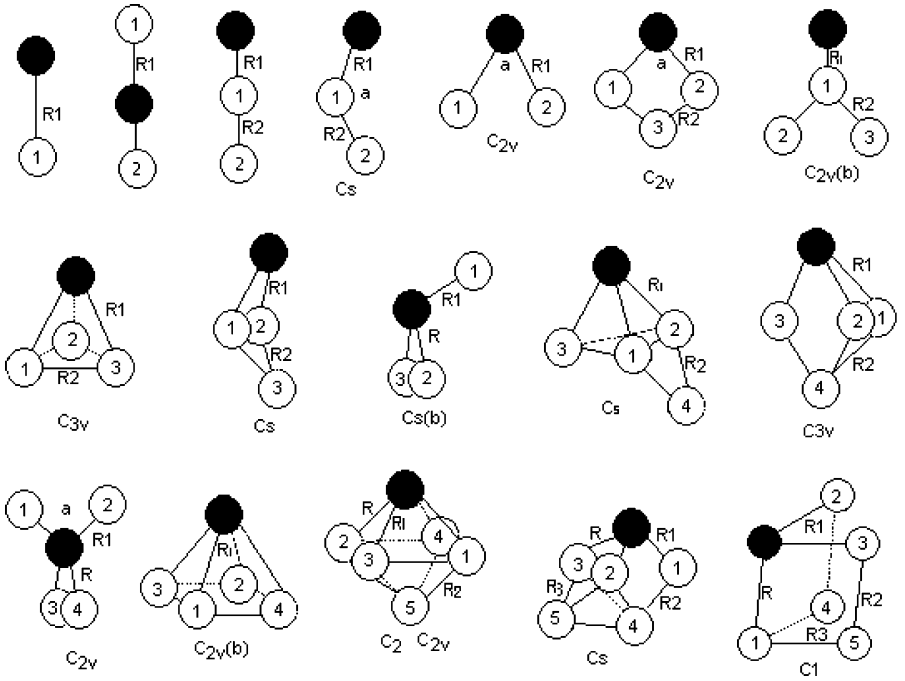

Figure 1. Structures of $ReSi_n$ ($n = 1-5$) clusters.

2.308, 2.301, and 2.252 Å, respectively; one notes that the Si−Si bond length is found to be elongated. Meanwhile, the total energies and Re−Si bond lengths decrease as the spin S goes from $S = 1/2$ to $S = 5/2$; therefore, the linear $C_{\infty v}$ $ReSi_2$ with $S = 5/2$ (spin sextet configuration), which is lower in total energy than the ones of the linear $C_{\infty v}$ and $D_{\infty h}$ isomers, corresponds to the most stable structure.

For the $ReSi_2$ cluster with C_{2v} symmetry, as can be seen from the findings related to the geometries of the examined systems, bond lengths and bond angles as well as total energies exhibit strong and obvious dependencies on the spin of the species considered; the Re−Si bond lengths of C_{2v} $ReSi_2$ as well as total energies increase, together with the steady drop in stability, while the SiReSi bond angle decreases as the spin S goes from $S = 1/2$ to 5/2 monotonically. This variation of bond length results from the charge-transfer (or interaction) among Re and silicon atoms. Thus, the $ReSi_2$ cluster with $S = 1/2$ is lower in total energy than those with spin $S = 3/2$ and 5/2; therefore, the C_{2v} $ReSi_2$ cluster with spin doublet configuration is the most stable structure.

The $ReSi_2$ cluster under the constraint of C_s symmetry, which is the distortion of $C_{\infty v}$ or C_{2v} isomers, is obtained. Geometry optimization on the bending $ReSi_2$ ($S = 1/2$, 3/2, and 5/2) cluster with C_s symmetry turns out to be the stable structure. On the basis of the SiSiRe bond angle (Table 1), we can find that the C_s $ReSi_2$ can be described as a slightly distorted $C_{\infty v}$ $ReSi_2$ cluster with the SiSiRe bond angle being about 178°. As can be seen from the findings related to the geometry correlation with the spin of the species considered, Re−Si bond lengths increase significantly while Si−Si bond lengths decrease as the spin S goes from $S = 1/2$, to $S = 3/2$, to $S = 5/2$. However, the theoretical result on total energies shows that $ReSi_2$ with $S = 3/2$ is lower in total energy than with $S = 1/2$ and 5/2; therefore, the Cs $ReSi_2$ cluster with spin quartet configuration is the most stable structure.

Theoretical analyses and discussions of geometries and stabilities of $ReSi_2$ clusters reveal that as the low-lying geometries of $ReSi_2$ clusters vary from $C_{\infty v}$, to C_s, to C_2v symmetry, the corresponding spin configurations of the stable $ReSi_2$ are 5/2 (spin sextet configuration), 3/2 (spin quartet configuration), and 1/2 (spin doublet configuration), respectively, and the corresponding total energies of $ReSi_2$ clusters with C_s, C_{2v}, and $C_{\infty v}$ symmetries are −86.6485, −86.7332, and −86.6653 hartrees, respectively. One notices that the C_{2v} $ReSi_2$ cluster with spin $S = 1/2$ is obviously the lowest-energy structure and is selected as the ground state; the corresponding electron state is $^2A_1$. Furthermore, the C_s isomer of $ReSi_2$ can be seen as intermediate between the C_{2v} $ReSi_2$ and $C_{\infty v}$ $ReSi_2$ forms.

$ReSi_3$. The possible $ReSi_3$ structures keeping D_{3h}, C_{2v}, C_s, and C_{3v} symmetries (Figure 1) with the spin of these species taken into account are investigated. The geometry structures are depicted at Figure 1. For the planar $ReSi_3$ (C_{2v}) cluster, the geometry can be seen as one silicon atom capped on the bottom of a $ReSi_2$ (C_{2v}) cluster. When spin S varies from $S = 1/2$, to $S = 3/2$, to $S = 5/2$, the Re−Si bond length is elongated while the Si(1)ReSi(2) bond angle decreases; meanwhile, the Si(1)−Si(3) (or Si(2)−Si(3)) bond length decreases monotonically. The elongation of the Re−Si bond length results from the weakness of the electrostatic interaction among Re and Si atoms. The harmonic vibrational frequency analysis on the C_{2v} $ReSi_3$ cluster indicates that $ReSi_3$ (C_{2v}) cluster with $S = 1/2$ displays an imaginary frequency, which corresponds to the transition state. Furthermore, a $ReSi_3$ cluster with spin $S = 3/2$ is lower in total energy than that with spin S = 5/2; therefore, $ReSi_3$ (C_{2v}) with $S = 3/2$ is more stable than that with spin $S = 5/2$. In addition, the most stable $ReSi_3$ (C_{2v}) cluster keeps the same spin quartet configuration as that of $ReSi_2$ (C_s) cluster.

Theoretical calculations of $ReSi_3$ (C_{2v}(b)) clusters with spin $S = 1/2$, 3/2, and 5/2 are performed at the UB3LYP/LanL2DZ level. Subsequently, the harmonic vibrational frequency analysis on $ReSi_3$ (C_{2v}(b)) clusters with doublet, quartet, and sextet spin configurations turns out to be the stable structures; furthermore, $ReSi_3$ (C_{2v}(b)) with spin $S = 5/2$ is lower in total energy than those with spin $S = 1/2$ and 3/2. Therefore, $ReSi_3$(C_{2v}(b)) with spin $S = 5/2$ is the most stable structure. Because the Re atom in $ReSi_3$ (C_{2v}(b)) clusters interacts with one silicon atom, in other words, two of the silicon atoms cap the bottom of the

TABLE 1: Geometries and Total Energies as Well as Relative Energies of $ReSi_n$ ($n = 1-12$) Clusters[a]

cluster	symm	spin	R_1/R	R_2	R_3	α	E_T	ΔE	E_b
ReSi	$C_{\infty v}$	1/2	2.203				−82.7756702	1.542	
		3/2	2.233				−82.832342	**0.000**	2.8485
		5/2	2.242				−82.7549391	2.106	
$ReSi_2$	$C_{\infty v}$	1/2	2.308	2.208		180.0	−86.5318073	5.479	
		3/2	2.301	2.227		180.0	−86.618366	3.123	
		5/2	2.252	2.233		180.0	−86.6652568	1.847	
	C_s	1/2	2.203	2.338		178.0	−86.642958	2.454	
		3/2	2.24	2.268		178.0	−86.6485016	2.303	
		5/2	2.439	2.204		177.8	−86.6122674	3.289	
	C_{2v}	1/2	2.231			78.6	−86.7331532	**0.000**	3.2924
		3/2	2.311			63.1	−86.6636337	1.892	
		5/2	2.545			52.3	−86.6232438	2.991	
	$D_{\infty h}$	1/2	2.343				−86.4670657	7.240	
		3/2	2.296				−86.2947712	11.928	
		5/2	2.322				−86.2150355	14.098	
$ReSi_3$	C_{2v}	3/2	2.330	2.359		101.7	−90.5633002	0.676	
		5/2	2.476			91.0	−90.5459759	2.110	
	C_{2v}(b)	1/2	2.384	2.334			−90.4492867	4.740	
		3/2	2.379	2.314			−90.4422801	4.931	
		5/2	2.549	2.248			−90.4699893	3.767	
	C_{3v}	1/2	2.304	2.910			−90.615975	0.205	
		3/2	2.235	3.363			−90.5646683	1.601	
	C_s	5/2	2.476	2.303		91.0	−90.545976	2.110	
	C_s(b)	1/2	2.269/2.261			94.4	−90.6235244	**0.000**	3.971
		3/2	2.245/2.268			100.3	−90.5646506	1.602	
$ReSi_4$	C_{2v}	3/2	2.262/2.345				−94.4832179	0.595	
	C_2v(b)	3/2	2.417/2.417				−94.4404136	1.759	
		5/2	2.539				−94.4223491	2.251	
	C_s	1/2	2.331	2.411		112.7	−94.5050705	**0.000**	3.3122
		3/2	2.350	2.465			−94.4610841	1.197	
		5/2	2.540	2.466		86.7	−94.4223483	2.251	
	C_{3v}	3/2	2.356	2.608			−94.4530529	1.415	
$ReSi_5$	C_2	1/2	2.413/2.415	2.657			−98.362557	0.217	
		3/2	2.443/2.511	2.480			−98.3338402	1.116	
	C_s	1/2	2.321/2.347	3.219	2.453		−98.3670347	0.213	
		3/2	2.348/2.370	3.205	2.470		−98.3573085	0.478	
	C_1	1/2	2.326/2.411	2.398	2.421		−98.3748573	**0.000**	3.6036
		3/2	2.447/2.444	2.764	2.674		−98.3281024	1.272	
		5/2	2.457/2.457	2.646	2.647		−98.3062587	1.867	
$ReSi_6$	C_s(a)	1/2	2.351				−102.2346734	1.160	
		3/2	2.362/2.396				−102.2422121	0.954	
	C_{2v}	1/2	2.493/2.351	3.559		59.6	−102.2346831	1.159	
	C_s	3/2	2.327/2.329				−102.2214506	1.519	
	C_1	1/2	2.34/2.35	2.54			−102.2473000	0.816	
		3/2	2.39/2.44	2.49			−102.2213433	1.522	
		5/2	2.37/2.40	3.40			−102.1903171	2.367	
	C_1(b)	1/2	2.384/2.384	2.400	2.400		−102.2772816	**0.000**	3.633
		3/2	2.820/2.872	2.690	2.464		−102.2206914	1.540	
	C_{2v}(b)	1/2	2.428/2.447				−102.2170074	0.824	
	C_s(b)	1/2	2.406/2.491	2.736	2.381		−102.2413213	0.163	
$ReSi_7$	C_1	1/2	2.402/3.967	2.455	2.478		−106.1407744	0.067	
		3/2	2.613/2.390	3.531	2.354		−106.0985174	1.217	
		5/2	2.497/2.540	3.862	3.186		−106.0796591	1.723	
	C_1(b)	1/2	2.482/2.437	2.406	2.336		−106.1432325	**0.000**	3.2441
		3/2	2.382/2.446	2.406	2.951		−106.1026121	1.105	
		5/2	2.397/2.463	2.415	2.533		−106.0671143	2.071	
$ReSi_8$	C_1	1/2	2.385/2.708				−110.0300273	**0.000**	3.2580
	C_1(b)	1/2	2.375/2.538	2.572			−110.0252869	0.129	
		3/2	2.297/2.538	2.482			−109.9981757	0.867	
		5/2	2.304/2.623	2.493			−109.9703688	1.623	
$ReSi_9$	C_1	1/2	2.770/2.902	2.494	3.735		−113.9396588	**0.000**	3.3378
		3/2	2.380/2.627	2.429	2.377		−113.8843472	1.505	
$ReSi_{10}$	C_1	1/2	2.363				−117.8118087	**0.000**	3.2998
		3/2	2.396				−117.7873343	0.666	
		5/2	2.486				−117.7523259	1.619	
	C_1(b)	1/2	2.668/2.632	2.400	2.731		−117.7988493	0.353	
		3/2	2.589/2.683	2.358	2.683		−117.781041	0.837	
		5/2	2.607/2.669	3.610	2.392		−117.7615224	1.368	

TABLE 1 (Continued)

cluster	symm	spin	R_1/R	R_2	R_3	α	E_T	ΔE	E_b
$ReSi_{11}$	C_s	1/2	2.427/2.701				−121.6579298	1.555	
	C_1(a)	1/2	2.615/2.561	2.440	2.343		−121.7150939	**0.000**	3.3454
		3/2	2.602/2.655	3.672	4.821		−121.6745109	1.104	
		5/2	2.626/2.622	2.448	2.420		−121.6474041	1.842	
	C_1(b)	1/2	2.427/2.701				−121.6579299	1.555	
		3/2	2.439/2.530	2.406	2.470		−121.6856556	0.801	
		5/2	2.472/2.622	2.389	2.467		−121.6557641	1.614	
	C_1(d)	1/2	2.681/2.453	2.413	2.383		−121.7150952	0.000	
		3/2	2.484/2.662	2.421	2.368		−121.6991675	0.433	
		5/2	2.524/2.725	2.499	2.446		−121.6576318	1.564	
$ReSi_{12}$	C_{2h}	1/2	2.690	2.392	2.461		−125.6405861	**0.000**	3.4340
	D_{6h}	1/2	2.690				−125.6405852	0.000	

[a] Units: the bond lengths are in Å, E_T is in hartree units, the relative energy ΔE and atomic averaged binding energy E_b are in eV. R_1 or R represent the Re−Si bond lengths, and R_2 and R_3 represent the Si−Si bond lengths (see Figures 1−3).

ReSi cluster. Consequently, the C_{2v}(b) $ReSi_3$ shows that the same spin sextet configuration as that of the linear $ReSi_2$ structure.

The possible geometries of $ReSi_3$ (D_{3h}, C_{3v}) clusters with spin $S = 1/2$, 3/2, and 5/2 are considered; however, theoretical results reveal that $ReSi_3$ (D_{3h}) turns out not to be a stable structure. After altering the localization of the Re atom, $ReSi_3$ (C_{3v}) is yielded. Specifically, the geometry of the $ReSi_3$ (C_{3v}) structure can be seen as the Re atom capping the planar Si_3 cluster and forming a trigonal pyramid; the Re atom interacts with three silicon atoms simultaneously with equivalent Re−Si bond lengths. $ReSi_3$ (C_{3v}) clusters with doublet spin configuration and quartet spin configuration are the stable structures. Unfortunately, theoretical results indicate that the $ReSi_3$ (C_{3v}) cluster with $S = 5/2$ is not a stable structure; after a relaxation of the geometry to a less symmetrical structure, a stable butterfly-like $ReSi_3$ (C_s) with $S = 5/2$ is finally yielded. On the basis of theoretical results of total energies on $ReSi_3$ (C_{3v}, C_s) clusters, it is found that $ReSi_3$ (C_{3v}) with spin $S = 1/2$ is more stable than those of $ReSi_3$ (C_{3v}, $S = 3/2$) and $ReSi_3$ (C_s, $S = 5/2$) clusters. Consequently, the C_{3v} $ReSi_3$ cluster with spin doublet configuration is the most stable geometry.

After the distortion of the C_{3v} isomer, the C_s(b) isomer is obtained. Theoretical results show that the C_s(b) isomer with spin doublet configuration is the most stable structure. Furthermore, the C_s(b) isomer with spin doublet spin configuration is 0.205 eV lower in total energy than the C_{3v} isomer with doublet spin configuration.

As a consequence of symmetries for the interesting low-lying isomers varying from C_{3v}, to C_{2v}, to C_{2v}(b), the energies of the corresponding isomers are −90.6160, −90.5633, and −90.4493 hartrees, respectively, together with the spin configuration going from spin doublet configuration to spin sextet configuration. On the basis of the theoretical results of geometries and total energies of the $ReSi_3$ (C_{3v}, C_s, C_s(b), C_{2v}(b), and C_{2v}) clusters above, it is obvious that $ReSi_3$ (C_s(b)) with spin $S = 1/2$ is the lowest-energy geometry; therefore, $ReSi_3$ (C_s(b)) with spin doublet configuration actually is the most stable structure and the ground state, with the corresponding electron state being $^2A'$. In addition, the C_2v isomer of $ReSi_3$ can be seen as intermediate between the C_2v(b) $ReSi_3$ and C_s(b) $ReSi_3$ forms.

$ReSi_4$. In analogy to the previous optimization results of $IrSi_4$ clusters,[9] theoretical calculations of $ReSi_4$ with C_{3v}, C_{2v}, and C_s symmetries (Figure 1) as the initial geometries considering of the spin electron configurations are carried out, followed by the harmonic vibrational frequency analysis. The C_{2v} $ReSi_4$ is the slight distortion of the unstable T_d isomer, and the Re atom localizes at the center site of Si_4 cluster and interacts actually with four silicon atoms simultaneously, which is the same as $IrSi_4$ (C_{2v} and C_2) clusters.[9] Geometry optimization of $ReSi_4$ (C_{2v}) cluster with spin $S = 1/2$, 3/2, and 5/2 is performed; however, the harmonic vibrational frequency analysis of the final results on $ReSi_4$ (C_{2v}) indicates that $ReSi_4$ (C_{2v}) with $S = 1/2$ and 5/2 has one imaginary frequency, which is corresponding to the transition state. Fortunately, theoretical results prove that $ReSi_4$ (C_{2v}, $S = 3/2$) is a thermodynamically stable structure.

The geometrical structure of $ReSi_4$ (C_{2v}(b)) can be described as the transition metal Re capping the distorted rhombus Si_4(C_{2v}) cluster and interacting with four Si atoms simultaneously. The harmonic vibrational frequency analysis on the $ReSi_4$ (C_{2v}(b)) cluster indicates that the $ReSi_4$(C_{2v}(b)) cluster with spin $S = 1/2$ has an imaginary frequency, which corresponds to the transition state. Theoretical results on total energies apparently reveal that $ReSi_4$ (C_{2v}(b)) with spin $S = 3/2$ is distinctly lower in total energy than that with spin $S = 5/2$. Therefore, $ReSi_4$ (C_{2v}(b)) with $S = 3/2$ is the most stable structure.

On the basis of the geometry of the stable C_{3v} $ReSi_3$ cluster above, the $ReSi_4$ (C_{3v}) cluster, which is selected as the candidate of the ground-state candidates, is yielded and can be characterized as one Si capped the bottom of the C_{3v} Si_3 plane (Figure 1). Theoretical results of geometry optimization and harmonic vibrational frequency analysis on $ReSi_4$ (C_{3v}) clusters reveal that only the $ReSi_4$ (C_{3v}, $S = 3/2$) cluster has no imaginary frequency, which corresponds to the low-lying structure.

As for the $ReSi_4$ cluster with C_s symmetry, this geometry is obtained by capping one silicon atom on the side of the $ReSi_3$ (C_{3v}) cluster (Figure 1), or this geometry can be seen as the distortion of the $ReSi_4$ (C_{3v}) cluster. The Re−Si (R_1) and Si−Si bond lengths as well as the total energies of $ReSi_4$ (C_s) cluster correlate with the spin configurations. As spin S goes from $S = 1/2$, to 3/2, to 5/2, the Re−Si (R_1) and Si−Si bond lengths are elongated, together with a pronounced drop of the stability of the C_s Si_4 cluster as the total energy of the C_s $ReSi_4$ cluster increases. One observes that the $ReSi_4$ ($S = 1/2$) cluster with C_s symmetry is the most stable structure.

As can be seen from the findings of total energies above, one finds that the $ReSi_4$ ($S = 1/2$) cluster with C_s symmetry, which is seen from Table 1, is the lowest one in total energy; therefore, it corresponds to the most stable structure among the investigated $ReSi_4$ clusters, with the corresponding electronic state being $^2A''$ character. In addition, the most stable C_s $ReSi_4$ with spin doublet configuration is the same as MSi_4 (M = Cr, Mo, W).[4,6,8] Furthermore, our theoretical results show that Re in the most stable $ReSi_4$ cluster favors absorbing on the surface site of the Si_4 cluster.

$ReSi_5$. The C_{2v} $ReSi_5$ geometry is obtained after the Si(5) atom is capped on the bottom of $ReSi_4$ (C_{2v}(b)) cluster. The

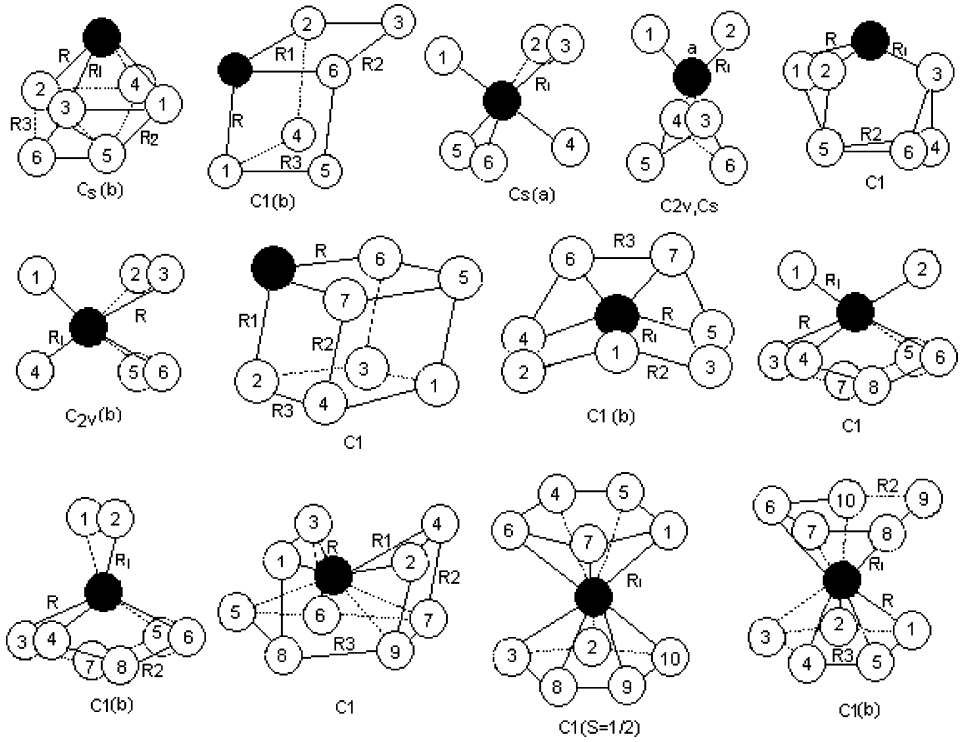

Figure 2. Structures of $ReSi_n$ ($n = 6-10$) clusters.

equilibrium geometry of C_{2v} $ReSi_5$ cluster is optimized at the UB3LYP/LanL2DZ level (Figure 2). The harmonic vibrational frequency analyses on the C_{2v} $ReSi_5$ cluster reveal that the C_{2v} $ReSi_5$ cluster turns out not to be a thermodynamically stable structure. After the C_{2v} $ReSi_5$ geometry undergoes the distortion into lower symmetry geometry, the thermodynamically stable C_2 $ReSi_5$ clusters with doublet and quartet spin states are obtained. The C_2 $ReSi_5$ cluster with spin sextet state is a transition state. On the basis of theoretical results on the C_{2v} $ReSi_5$ cluster, Re−Si bond lengths in the C_2 $ReSi_5$ cluster are associated with the spin configurations. The Re−Si bond lengths as well as total energies of the $ReSi_5$ (C_2) cluster increase, together with drops of the stability and electrostatic interactions of Re and Si atoms monotonically, as the spin varies from $S = 1/2$ to $S = 3/2$. Therefore, the $ReSi_5$ (C_2) cluster with doublet spin configuration is the most stable structure.

The geometry of the C_s $ReSi_5$ cluster as the most likely candidate for the ground state geometry is yielded after the Si-(5) atom is capped on the side of the $ReSi_4$ (C_{3v}) cluster, and theoretical results on the $ReSi_5$ cluster with C_s symmetry apparently show that Re−Si bond lengths (R_1 and R) and Si−Si bond lengths (R_2 and R_3) along with the total energy of the C_s $ReSi_5$ cluster increase as spin S goes from $S = 1/2$ to $S = 5/2$ steadily. However, the $ReSi_5$ (C_s) with $S = 5/2$ turns out not to be a stable structure. Furthermore, the Re atom in the stable $ReSi_5$ isomers absorbs on the surface site of the Si_5 cluster, and $ReSi_5$ (C_s) with spin $S = 1/2$ is 2.98 kcal/mol lower in total energy than the $ReSi_5$ (C_2) cluster with spin $S = 1/2$, reflecting the higher stability of the C_s $ReSi_5$ ($S = 1/2$) as compared with the C_2 $ReSi_5$ ($S = 1/2$) cluster.

A C_1 $ReSi_5$ cluster, which can be described as Re replacing one of the silicons in distorted D_{3h} Si_6 cluster, is considered. Re−Si bond lengths and total energies are associated with the spin of this species. Theoretical results show that the C_s $ReSi_5$ cluster is 0.213 eV higher in total energy than the C_1 $ReSi_5$ cluster. Therefore, $ReSi_5$ (C_1) with spin doublet state is the most stable structure, and the Re atom absorbs on the surface of the silicon frame.

$ReSi_6$. Identified equilibrium geometries of $ReSi_6$ clusters with O_h, C_{5v}, C_{2v}, C_s, and C_1 point-group symmetries (Figure 2), taking into account spin electron configurations, are optimized at the UB3LYP level, followed by the harmonic vibrational frequency analyses. Theoretical results of $ReSi_6$ clusters with C_1 symmetry are listed at Table 1 with the figure depicted in Figure 2. By inspecting the data indicated in Tables 1 and 2, which summarize the essential geometries and electronic features of $ReSi_6$ clusters, one notices that the stable C_1 $ReSi_6$ cluster, with the transition metal Re capped the top of Si_6 cluster, is a slight distortion of D_{3d} symmetry. Theoretical results (Table 1) show that the total energies of C_1 $ReSi_6$ clusters correlate with spin configurations; in other words, the total energies increase steadily as the spin goes from 1/2 to 5/2. Therefore, the C_1 $ReSi_6$ with spin doublet state is the most stable structure. After an arrangement of the C_1 $ReSi_6$ isomer, the C_1(b) $ReSi_6$ isomer, which can be seen as one silicon capped on the C_1 $ReSi_5$ isomer, is more stable than its C_1 $ReSi_6$ isomer.

On the basis of the equilibrium geometry of the C_s(a) $ReSi_6$ cluster, the C_s(a) $ReSi_6$ structure can be depicted as a transition metal atom doped into the Si_6 cluster with a slight distortion of the unstable geometry of O_h and D_{3d} symmetries. It is not surprising that the total energy is correlated with the spin electron configurations. Furthermore, the total energies decrease as the spin S goes from spin doublet configuration to spin quartet configuration. Unfortunately, the geometry with spin sextet spin configuration is a transition state. Therefore, the isomer with the spin quartet configuration is the most stable structure. After the rearrangement of C_s(a) $ReSi_6$ geometry, the $ReSi_6$ cluster with C_{2v}(b) is yielded with the Re atom localizing at the center of Si_6 cluster and having a tendency to interact with all silicon atoms with nonequivalent bond lengths. Theoretical results of vibrational frequency analyses verify that only the $ReSi_6$ with spin doublet configuration is the stable structure.

After adjustment of C_s(a) $ReSi_6$ geometry above, the C_{2v} $ReSi_6$ cluster is yielded with the Re atom interacting with four silicon atoms simultaneously. The C_{2v} $ReSi_6$ geometry may be interpreted as a deformed substitutional structure, derivable from

TABLE 2: Natural Populations and Natural Electron Configurations of Re in $ReSi_n$ ($n = 1-12$) Clusters

cluster	symm	spin	natural population	natural electron configuration 6s	5d	6p	7s	6d
ReSi	$C_{\infty v}$	1/2	−0.1736	1.08	6.09	0.02		
		3/2	−0.0790	1.08	5.98	0.02		
		5/2	0.1009	0.80	6.03	0.08		
$ReSi_2$	$C_{\infty v}$	1/2	0.0619	0.67	6.20			
		3/2	0.1395	0.78	6.09	0.01		
		5/2	0.2806	0.85	5.87	0.02		
		1/2	0.0619	0.67	6.28			
		3/2	0.1807	0.84	5.98	0.01	0.01	
		5/2	0.3234	0.86	5.81	0.02	0.01	
	C_{2v}	1/2	−0.5402	0.88	6.65	0.03		
		3/2	−0.0769	0.79	6.25	0.05		
		5/2	0.1894	0.75	6.02	0.04		
	$D_{\infty h}$	1/2	−1.2432	0.82	7.43	0.01		
		3/2	−1.2902	1.28	7.01	0.01		
		5/2	−1.0263	0.74	7.31	0.01	0.01	
$ReSi_3$	C_{2v}	3/2	−0.0753	0.74	6.30	0.05	0.01	
		5/2	0.2541	0.87	5.82	0.06	0.01	
	C_{3v}	1/2	−0.7191	0.76	6.91	0.06	0.01	
		3/2	−0.9083	0.51	7.38	0.03	0.01	
	C_s	5/2	0.2543	0.87	5.82	0.06		
	C_{2v}(b)	1/2	0.1854	1.31	5.50	0.01		
		3/2	0.1996	1.28	5.52	0.01		
		5/2	0.5471	1.11	5.31	0.03	0.01	
	C_s(b)	1/2	−0.8854	0.73	7.11	0.05	0.01	
		3/2	−0.8463	0.59	7.23	0.03	0.01	
$ReSi_4$	C_{2v}	3/2	−1.3363	0.74	7.55	0.05	0.02	
	C_{2v}(b)	3/2	−0.5489	0.59	6.86	0.11	0.01	
		5/2	−0.0716	0.61	6.37	0.10	0.02	
	C_s	1/2	−0.7584	0.61	7.08	0.08	0.01	
		3/2	−0.5877	0.74	6.80	0.06	0.01	
		5/2	−0.0692	0.61	6.36	0.10	0.02	
	C_{3v}	3/2	−0.4613	0.78	6.62	0.07	0.01	
$ReSi_5$	C_2	1/2	−0.5094	0.69	6.68	0.14	0.01	
		3/2	−0.2917	0.64	6.56	0.10	0.02	
	C_s	1/2	−0.6400	0.56	6.99	0.10	0.01	
		3/2	−1.3010	0.68	7.56	0.06	0.02	
	C_1	1/2	−0.6966	0.50	7.11	0.09	0.01	
		3/2	−0.7429	0.51	7.15	0.10	0.01	
		5/2	−0.7537	0.61	7.05	0.01	0.02	
$ReSi_6$	C_s(a)	1/2	−1.8734	0.73	8.06	0.08	0.01	
		3/2	−1.2034	0.62	7.49	0.09	0.02	
	C_{2v}	1/2	−1.8732	0.73	8.06	0.08	0.01	
	C_s	3/2	−1.5428	0.68	7.79	0.07	0.02	
	C_1	1/2	−0.7916	0.70	6.98	0.11	0.01	
		3/2	−0.5300	0.58	6.84	0.11	0.02	
		5/2	−1.1160	0.64	7.38	0.09	0.02	
	C_1(b)	1/2	−0.5641	0.51	6.93	0.12	0.02	
		3/2	−0.6311	0.65	6.88	0.11	0.01	
	C_{2v}(b)	1/2	−1.3826	0.68	7.60	0.10	0.02	
	C_s(b)	1/2	−0.5619	0.66	6.76	0.15	0.02	
$ReSi_7$	C_1	1/2	−0.6532	0.65	6.86	0.16	0.02	
		3/2	−0.7239	0.52	7.05	0.15	0.02	
		5/2	−0.8077	0.63	7.03	0.15	0.02	
	C_1(b)	1/2	−0.8177	0.51	7.20	0.09	0.04	
		3/2	−1.0791	0.57	7.42	0.07	0.04	
		5/2	−0.7072	0.53	7.07	0.10	0.04	
$ReSi_8$	C_1	1/2	−1.2550	0.53	7.58	0.12	0.03	
	C_1(b)	1/2	−1.2530	0.59	7.51	0.14	0.01	0.03
		3/2	−1.6452	0.64	7.88	0.11	0.02	
		5/2	−1.6679	0.66	7.89	0.10	0.01	0.02
$ReSi_9$	C_1	1/2	−1.3922	0.55	7.67	0.16	0.01	0.03
		3/2	−1.3510	0.57	7.62	0.14	0.01	0.03
$ReSi_{10}$	C_1	1/2	−1.5683	0.55	7.83	0.17	0.01	0.03
		3/2	−1.7096	0.55	7.97	0.16	0.01	0.03
		5/2	−1.7981	0.54	8.10	0.11	0.01	0.06
	C_1(b)	1/2	−1.5664	0.54	7.82	0.17	0.01	0.03
		3/2	−1.3676	0.53	7.65	0.16	0.01	0.03
		5/2	−1.3403	0.54	7.60	0.16	0.01	0.05
$ReSi_{11}$	C_s	1/2	−1.6213	0.51	7.91	0.18	0.01	0.03
	C_1(a)	1/2	−1.5986	0.50	7.90	0.16	0.01	0.03
		3/2	−1.7122	0.51	8.00	0.16	0.01	0.03
		5/2	−1.7382	0.53	8.00	0.17	0.01	0.03
	C_1(b)	1/2	−1.6210	0.51	7.91	0.18	0.01	0.03
		3/2	−1.8103	0.49	8.11	0.17	0.01	0.03
		5/2	−1.6211	0.50	7.93	0.15	0.01	0.03
	C_1(d)	1/2	−1.5987	0.50	7.90	0.16	0.01	0.03
		3/2	−1.6526	0.53	7.93	0.16	0.01	0.03
		5/2	−1.5572	0.50	7.85	0.16	0.01	0.04
$ReSi_{12}$	C_{2h}	1/2	−1.3503	0.44	7.67	0.17	0.02	0.05
	D_{6h}	1/2	−1.3496	0.44	7.67	0.17	0.02	0.05

the O_h ground state of Si_7 through replacement of one Si atom by Re. Geometry optimization on the $ReSi_6$ cluster with C_{2v} symmetry reveals that only the geometry with spin doublet configuration is found to be the stable structure. After relaxation of the C_{2v} geometry with spin quartet configuration along the imaginary frequency, the new structure with C_s symmetry is found. The harmonic vibrational frequency analysis on the C_s isomer proves that the C_s isomer with spin quartet configuration is a stable structure.

The $ReSi_6$ cluster with C_{5v} symmetry, which arises from the replacement of the Si atom by the Re atom in the D_{5h} Si_7 isomer, is taken into account. Harmonic vibrational frequency analysis shows that the C_{5v} $ReSi_6$ cluster is an unstable structure. This C_s(b) $ReSi_6$ structure, which results from geometry optimization of the distorted C_{5v} $ReSi_6$ isomer, can be seen as one silicon atom capped the side of the C_2 $ReSi_5$ cluster; furthermore, the Re atom absorbs on the surface site of the silicon cluster. The final theoretical result shows that only the C_s(b) $ReSi_6$ with spin doublet configuration is the stable structure. The C_s(b) $ReSi_6$ with quartet and sextet spin configurations is the transition state.

According to the theoretical analysis above, it should be noted that the Re atom in most of the stable $ReSi_6$ isomers tends to localize at the center site of Si_6 cluster and interacts with all silicon atoms simultaneously. However, on the basis of theoretical results of total energies for $ReSi_6$ clusters with C_{2v}, C_s, and C_1 symmetries (Table 1), it is apparent that the $ReSi_6$ (C_1(b), $S = 1/2$) cluster with the Re atom absorbing on the surface site of the Si_6 cluster is lower in total energy than that of the $ReSi_6$ (C_s(a), $S = 3/2$) cluster with the Re atom localizing at the center site of the Si_6 frame. The $ReSi_6$ (C_1(b)) cluster with spin doublet configuration turns out to be the most stable structure.

$ReSi_7$. The possible geometries of $ReSi_7$ clusters under the constraint of C_{3v}, D_{5h}, and C_1 symmetries are considered. Theoretical results show that the C_{3v} and D_{5h} $ReSi_7$ isomers with Re localizing at the center of silicon atoms are not the stable structures; however, the equilibrium geometry with C_1 symmetry is proven to be a stable structure. Specifically, this C_1 $ReSi_7$ geometry can be seen as Re replacing one of the Si atoms in a slightly distorted C_{4v} Si_8 cluster, or it can be described as one silicon atom capped the bottom of the most stable C_1 $ReSi_6$ isomer. The total energies of C_1 $ReSi_7$ and natural populations of Re atom increase, when spin S varies from 1/2 to 5/2, reflecting that the C_1 $ReSi_7$ isomer with doublet spin configuration is the most stable structure. Furthermore, theoretical results reveal that the Re atom in C_1 $ReSi_7$ favors absorbing on the surface of the silicon frame and bringing out the stable structure of the C_1 $ReSi_7$ isomer.

The interesting butterfly-like C_1(b) $ReSi_7$ cluster is obtained after the rearrangement of the D_{5h} $ReSi_7$ geometry, the structure can be described as Re capped the distorted planar structure. The Re atom interacts with all silicon atoms simultaneously with nonequivalent bond lengths, and the Si(6) and Si(7) atoms

deviate to distorted planar. It is worth noting that the Re atom in the C_1(b) $ReSi_7$ cluster has a trend to absorb on the surface site of the Si_7 cluster. Re−Si(5) and Si(1)−Si(3) bond lengths increase as the spin S varies from $S = 1/2$ to $S = 5/2$. On the basis of the theoretical results of total energies on the C_1(b) $ReSi_7$ cluster, it should be noted that the total energies are correlated with the spin configurations. This feature is shown to be associated with a pronounced drop in the stability of the cluster as the spin goes from doublet, to quartet, to sextet spin configurations. It is worth pointing out that the C_1(b) $ReSi_7$ cluster with doublet spin configuration corresponds to the most stable structure.

In general, it should be noted that, for $ReSi_7$, two isomers are found, namely C_1 $ReSi_7$ ($S = 1/2$) and C_1(b) $ReSi_7$ ($S = 1/2$) isomers, differing in total energy about 0.067 eV; therefore, C_1(b) $ReSi_7$ with $S = 1/2$ is the most stable structure. In addition, Re in the lowest-energy $ReSi_7$ isomer prefers the surface site to the center site.

$ReSi_8$. Initial configurations of Si_8Re clusters, maintaining D_{4h}, D_{4d}, C_{3v}, C_{2v}, and C_1 symmetries, are considered as the possible candidates of the ground state geometry. The harmonic vibrational frequency analysis on Si_8Re clusters with D_{4h}, D_{4d}, C_{3v}, and C_{2v} symmetries shows that they are not the thermodynamically stable structures. However, after the distortion of the geometry according to the imaginary coordinate, the Si_8Re clusters with C_1(b) and C_1 symmetries, which distort slightly the C_{2v} geometry, are yielded (Figure 2). Initial geometries of the slightly distorted C_1 $ReSi_8$ and C_1(b) $ReSi_8$ clusters with Re absorbing on the surface site are taken into consideration and optimized; however, the final equilibrium geometry proves that the Re atom moves from the surface site to the center site, and the Re localizes at the center site of the Si_8 frame and interacts with all silicon atoms simultaneously with nonequivalent bond lengths. In other words, the Re atom is surrounded by Si atoms, and this result shows that Re prefers the center site to the surface site. This behavior of Re in C_1(b) and C_1 $ReSi_8$ clusters is different from that of $ReSi_n$ ($n < 8$). Theoretical results show that R_1 or R bond lengths and the total energy of the C_1(b) Si_8Re cluster correlate with the spin configurations; in other words, the R_1 or R bond lengths along with total energy of C_1(b) Si_8Re cluster increase as the spin S goes from $S = 1/2$ to $S = 5/2$. Therefore, C_1(b) $ReSi_8$ with the doublet spin configuration is the most stable structure. Furthermore, the C_1 Si_8Re cluster is lower in total energy by about 0.128 eV than C_1(b) $ReSi_8$; consequently, the C_1 Si_8Re cluster with doublet spin configuration is energetically the most stable structure. Anyway, this result gives firm support to our previous prediction[2] and our conclusion that the Re atom tends to be trapped in the silicon cage in the $ReSi_n$ ($n > 7$) cluster. In fact, this phenomenon of the TM tending to localize at the center site of Si frame is found in some subunits of small $IrSi_n$ ($n = 4-6$)[9] and $CuSi_x$.[29]

$ReSi_9$. The $ReSi_9$ geometry with C_1 symmetry is taken into consideration. The C_1 $ReSi_9$ cluster is composed of Si_4 and Si_5 units. Specifically, this structure can be seen as one silicon atom being removed from the slightly distorted C_1(b) $ReSi_{10}$ cluster or can be described as one silicon atom capped the side of C_1(b) $ReSi_8$ isomer. The Re atom localizes at the center of Si_9 cluster and interacts with all silicon atoms with nonequivalent bond lengths. Theoretical results show that the C_1 $ReSi_9$ clusters with spin $S = 1/2$, 3/2, and 5/2 are the stable clusters. The Re atom in the stable C_1 $ReSi_9$ with $S = 1/2$, 3/2, and 5/2 carries −1.39e, −1.35e, and −1.30e, respectively; the electrostatic interactions among Re and Si atoms of doublet spin configuration are stronger than those for the quartet and sextet spin configurations. Therefore, the Re atom in the C_1 $ReSi_9$ cluster plays an important role in stabilizing the cluster. One should notice that Si(5)−Si(8) and Si(5)−Si(6) bond lengths in the C_1 $ReSi_9$ cluster with doublet configuration are 2.337 and 2.343 Å, shorter than R_2 and R_3 bond lengths, respectively. Furthermore, the Si(5) atom in the C_1 $ReSi_9$ cluster deviates slightly the planar Si_5 units. It is worth noting that the R and R_3 bond lengths in the C_1 $ReSi_9$ cluster are elongated; meanwhile, the total energy of C_1 $ReSi_9$ cluster increases, together with steady dropping of the stability, as the spin S varies from $S = 1/2$ to 5/2. In addition, harmonic vibrational frequency analysis proves that C_1 $ReSi_9$ with sextet spin configuration is a transition state. It obviously indicates that the C_1 $ReSi_9$ with doublet spin configuration is the most stable structure.

$ReSi_{10}$. The metal atom in sandwichlike $ReSi_{10}$ plays a role in terminating the dangling bonds of silicon atoms and should therefore be localized at the center of the Si_{10} frame in order to interact with all of the atoms equivalently. Equilibrium geometries of the sandwichlike $ReSi_{10}$ clusters with higher symmetry are optimized; however, the harmonic vibrational frequency analyses on the $ReSi_{10}$ cluster turn out not to be the stable structures (Figure 2). After relaxation of the geometry along with the imaginary frequency coordinate, the stable $ReSi_{10}$ (C_1) cluster with spin $S = 1/2$, 3/2, and 5/2 is found. The theoretical result of geometrical structure manifests that cagelike $ReSi_{10}$ (C_1) slightly deviates from the $FeC_{10}H_{10}$-like structure. Theoretical results on equilibrium geometry indicate that the Si(1)−Re bond lengths are elongated and total energies increase while the spin S goes from $S = 1/2$ to $S = 5/2$. Consequently, $ReSi_{10}$ (C_1, $S = 1/2$) turns out to be the most stable structure. In addition, the charge transfer among Re and silicon atoms significantly increases the stability of the C_1 $ReSi_{10}$ cluster.

The initial geometry of the C_1(b) $ReSi_{10}$ cluster with a transition metal atom localizing on top of the Si_{10} frame, which can be specifically described as one silicon atom capping the side of the C_1 $ReSi_9$ isomer, is considered. One notices that the transition metal Re finally moves from surface site to center site and localizes at the center site of the Si_{10} frame after the full geometry optimization. The Re atom interacts with all silicon atoms and tends to accept more charges from silicon atoms, and Re makes an important contribution to the stability of the Si_{10} frame. This geometry can be described as one silicon atom capped the C_1 $ReSi_9$ cluster or the slightly distorted sandwichlike D_{5h} $ReSi_{10}$ isomer with the Re atom interacting with all silicon atoms with nonequivalent bond lengths. On the basis of total energies of the C_1(b) $ReSi_{10}$ cluster, theoretical results show that the C_1(b) $ReSi_{10}$ cluster with the spin of this species considered turns out to be the energetic stable structure; furthermore, the C_1(b) $ReSi_{10}$ isomer with doublet spin configuration is the most stable structure.

Two isomers, namely C_1(a) $ReSi_{10}$ and C_1(b) $ReSi_{10}$ isomers, are investigated, and theoretical results show that the C_1(a) $ReSi_{10}$ isomer with doublet spin configuration is 0.353 eV lower in total energy than its C_1(b) $ReSi_{10}$ isomer with doublet spin configuration; consequently, the C_1(a) $ReSi_{10}$ isomer is the lowest-energy structure, which corresponds to the ground state. According to our previous theoretical results[2] and the final equilibrium geometry of $ReSi_{10}$ clusters, one can find that $TMSi_n$ with TM inserting into the Si_n frame is lower in total energy than that with TM absorbing on the surface of the Si_n frame. In other words, the $TMSi_n$ with TM inserting into Si_n frame is more stable than that with TM absorbing on the surface of Si_n frame. Perhaps this theoretical phenomena discussed above can

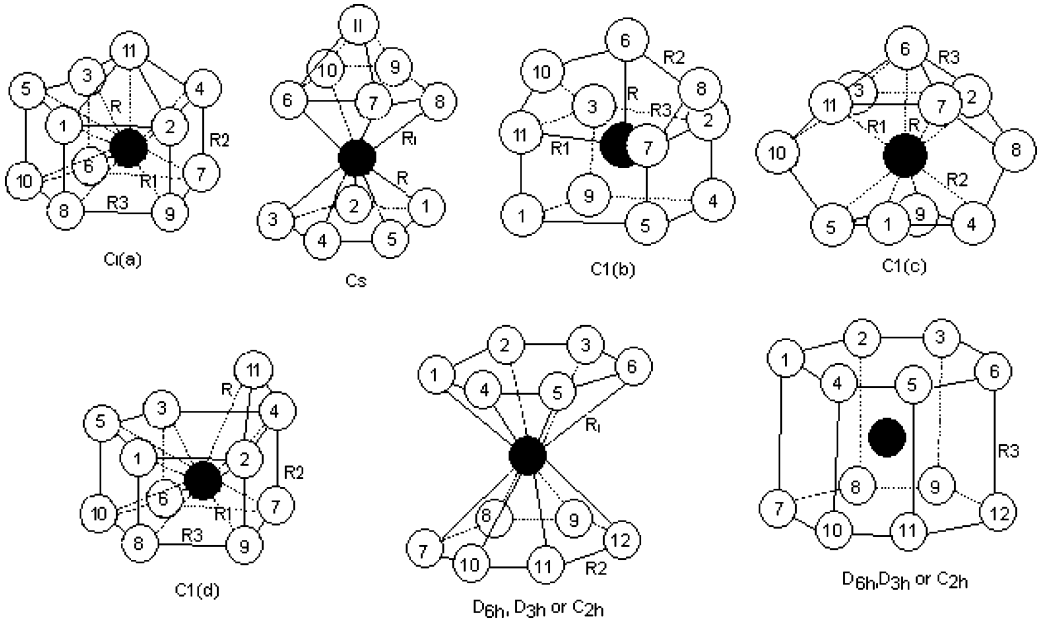

Figure 3. Structures of $ReSi_n$ ($n = 11, 12$) clusters.

give an interpretation of experimental observation of TM preferring to insert into Si bulk.[30]

$ReSi_{11}$. According to the theoretical result of the sandwichlike C_1(b) $ReSi_{10}$ cluster above, the C_1(a) $ReSi_{11}$ cluster is yielded after one silicon atom is capped on the top of the C_1(b) $ReSi_{10}$ cluster. The Re atom in the C_1(a) $ReSi_{11}$ cluster interacts with all silicon atoms simultaneously (Figure 3). Specifically, this structure is the slightly distorted C_{5v} $ReSi_{11}$ isomer. The theoretical result on the C_1(a) $ReSi_{11}$ cluster turns out to be the stable structure. Si(11)−Re bond lengths in C_1(a) $ReSi_{11}$ isomers with doublet, quartet, and sextet spin configurations are 2.453, 2.432, and 2.423 Å, respectively. It is apparently shown that the Si(11)−Re bond length and total energy of the C_1(a) $ReSi_{11}$ cluster depend on the spin of this species. The decrease of the Si(11)−Re bond length and the steady increase of total energy are found. This feature is shown to be associated with pronounced drop in the stability of the C_1(a) $ReSi_{11}$ cluster as spin S varies from $S = 1/2$ to $5/2$.

Guided by the geometry of the C_1(b) $ReSi_{10}$ cluster above, the $ReSi_{11}$ cluster with well-defined C_{5v} symmetry considering spin configurations is taken into account. Specifically, this structure can be seen as one silicon atom capped the top of the D_{5d} $ReSi_{10}$ cluster with Re atom localizing at the center of Si_{10} cage. The Re atom interacts with all silicon atoms simultaneously and terminates the dangling bonds of the Si frame. Unfortunately, geometry optimization on the C_{5v} $ReSi_{10}$ cluster turns out to be an unstable structure. After distortion of the geometry along the imaginary coordinate, the C_s $ReSi_{11}$ cluster is yielded (Figure 3). Harmonic vibrational frequency analysis on the C_s $ReSi_{11}$ cluster with doublet spin configuration turns out to reveal that this is the stable structure, while the shortest Re−Si(11) bond length is 2.410 Å. Unfortunately, the C_s $ReSi_{11}$ clusters with quartet and sextet spin configurations have some imaginary frequencies, which are not the stable structures. However, after the rearrangement of the C_s $ReSi_{11}$ cluster, the stable C_1(b) $ReSi_{11}$ cluster is yielded. Specifically, the geometry is seen as the slightly distorted C_{2v} $ReSi_{11}$ cluster with Re localizing at the center of the Si_{11} frame and interacting with all atoms simultaneously. The Re−Si(11) (R_1) bond length in the C_1(b) $ReSi_{11}$ cluster is elongated as the spin S goes from $S = 1/2$ to $5/2$; theoretical results show that the C_1(b) $ReSi_{11}$ with quartet spin configuration is the most stable structure.

According to geometries on the stable Si_{11} isomers,[31] initial C_1(c) geometry with Re inserting into Si_{11} frame is considered. However, the final theoretical result of optimized equilibrium geometry reveals that the C_1(d) isomer with spin doublet spin configuration is the most stable isomer; furthermore, the total energy of the C_1(d) isomer is only a little lower than the C_1(a) isomer. However, because the energy difference between both the C_1(a) and C_1(d) isomers is very small (0.01 meV), these isomers are considered as the degenerate structures.

On the basis of the total energies of $ReSi_{11}$ isomers summarized in Table 1 and the theoretical analysis above, it is worthwhile pointing out that the coordination number of C_s, C_1(a), C_1(b), and C_1(d) isomers is 11. Furthermore, the C_1(d) $ReSi_{11}$ cluster with doublet spin configuration is the lowest-energy structure, which is selected as the ground state configuration. Theoretical results on $ReSi_{11}$ cluster reveal that Re in $ReSi_{11}$ isomer prefers the center site, which demonstrates our prediction again.[2]

$ReSi_{12}$. According to the analysis on sandwichlike $ReSi_{10}$ above and the previous results on WSi_{12}, $CuSi_{12}$ clusters,[6,16,29,32] and $RuSi_{10}$ as well as $ReSi_{11}$ above, the possible geometries of sandwichlike $ReSi_{12}$ are considered with the transition metal placed at the center site of Si_{12} frame and interacting with all the silicon atoms simultaneously (Figure 3). Therefore, geometry optimizations of $ReSi_{12}$ clusters with well-defined C_{2h}, D_{6h}, and D_{3h} point-group symmetries are performed at the UB3LYP/LanL2DZ level taking into consideration the spin configurations, followed by the harmonic vibrational frequency analysis. Theoretical results indicate that $ReSi_{12}$ cluster with D_{3h} symmetry has an imaginary frequency, which corresponds to a transition state. However, $ReSi_{12}$ clusters with D_{6h} and C_{2h} symmetries turn out to be the stable structures; furthermore, $ReSi_{12}$ with C_{2h} symmetry is slightly lower in total energy than its isomer with D_{6h} symmetry. Thus, the sandwichlike $ReSi_{12}$ structure with C_{2h} symmetry is considered as a degenerate structure of the D_{6h} isomer. Re acts as an acceptor and carries −1.35e, and this contributes to the stability of the C_{2h} $ReSi_{12}$ cluster. Furthermore, the coordination number in the C_{2h} isomer is 12, and the corresponding electronic state of C_{2h} isomer is ^{2}Ag character. The sandwichlike $ReSi_{12}$ geometry, which is the same as the WSi_{12} cluster[6] in our previous paper, is considered

as one of the smaller cage, and it can be seen as the smaller building block of material.

3.2. Population Analysis. On the ground of natural populations and natural electron configurations of $ReSi_n$ ($n = 1-12$) clusters summarized at Table 2, we will describe the charge transfer of $ReSi_n$ ($n = 1-12$) clusters in the following subsection. It is interesting to find that the natural populations of Re atom in the most stable $ReSi_n$ ($n = 1-12$) depend on spin configurations of this species considered. The charges of ReSi, $ReSi_2$ (C_{2v}), and $ReSi_3$ (C_{2v} and C_{3v}) clusters with doublet and quartet spin configurations transfer from Si atoms to Re atom. The Re atom in ReSi, C_{2v} $ReSi_2$, and C_{2v} and C_{3v} $ReSi_3$ clusters with spin $S = 1/2$ and 3/2 acts as an acceptor and can enhance the stability; therefore, the Re−Si bond lengths of C_{2v} $ReSi_2$ with $S = 1/2$ are shorter than the others. On the contrary, the charges of ReSi, $ReSi_2$ (C_{2v}), and $ReSi_3$ (C_{2v} and C_{3v}) clusters with sextet spin configuration are transferred from Re to Si. In addition, the natural population of 5d orbitals of Re for the most stable $ReSi_n$ ($n = 1-3$) isomers is about 6, and one charge in the most stable ReSi and $ReSi_2$ clusters is transferred from 6s of Re to 5d orbitals of the Re atom. The natural populations of Re atoms in $ReSi_2$ (C_s and $C_{\infty v}$) clusters with doublet, quartet, and sextet spin configurations are positive, and the charges of $ReSi_2$ (C_s and $C_{\infty v}$) isomers transfer from Re atom to Si atoms, which are different from those of MSi_n (M = Mo, W, and Ir) clusters. Furthermore, the charges in $ReSi_n$ ($n = 4-12$) clusters transfer from silicon atoms and 6s orbitals of the Re atom to 5d orbitals of Re atom, and the charge transfer of the most stable $ReSi_n$ ($n = 4-12$) clusters steadily decreases as spin S goes from $S = 1/2$ to 5/2. The natural population of 5d orbitals of Re in the most stable $ReSi_n$ ($n = 3-7$) is about 7, and the natural population of 5d orbitals of Re in the most stable $ReSi_n$ ($n = 8-12$) is about 8. The Re atom in C_1(b) $ReSi_{11}$ carries −1.62e, −1.81e, and −1.62e for spin $S = 1/2$, 3/2, and 5/2, respectively, which acts as an acceptor of charge. It obviously shows that charges transfer from Si atoms to Re, and the natural population of Re in C_1(b) $ReSi_{11}$ with quartet spin configuration is bigger than the ones with doublet and sextet spin configurations. Furthermore, the electrostatic interactions among Re and Si atoms depend on the charge transfer among Re and silicon atoms. Consequently, the electrostatic interaction of Re and Si atoms in C_1(b) $ReSi_{11}$ with quartet spin configuration is stronger than those with doublet and sextet spin configurations due to the contribution of charge transfer in the C_1(b) $ReSi_{11}$ cluster. It is no wonder that C_1(b) $ReSi_{11}$ ($S = 3/2$) is the most stable structure. In general, the natural population of 5d orbitals of Re for the most stable $ReSi_n$ ($n = 1-12$) isomers increases, but on the contrary, the natural population of the 6s orbital of Re atom in the most stable $ReSi_n$ ($n = 1-12$) isomers decreases, as the number of Si atoms increases. Also, the natural populations of Re in the most stable $ReSi_n$ ($n = 1-12$) isomers are negative, and as charges are transferred from silicon atoms to Re atom, Re acts as an acceptor. The charge transfer among Re and Si atoms in the most stable $ReSi_n$ ($n = 1-12$) isomers does contribute to the stability of the species investigated. In addition, the charge transfer from Si and 6s orbitals of Re to 5d orbitals to Re degrades the efficiency of Si semiconductor after Re inserts into Si frame, which is in good agreement with our previous theoretical calculation and experimental observation.[2,33] Furthermore, the natural population of Re atom in the low-lying stable $ReSi_n$ ($n = 1-12$) clusters is influenced by the spin configurations.

3.3. Fragmentation Energy and Atomic Averaged Binding Energy. The fragmentation energy of the most stable $ReSi_n$ ($n = 1-12$) clusters with respect to removal of one Si atom is calculated at the UB3LYP/LanL2DZ level. A systematical investigation on MSi_n (M = Cr, Mo, W, Ir; $n = 1-6$) clusters shows that the density functional method (UB3LYP) in conjunction with LanL2DZ basis sets yields reasonable results.[6,8,29] The exchange-correlation energies are considered completely by the UB3LYP method during the calculations of $ReSi_n$ ($n = 1-12$) clusters.

In a further series of investigations, we evaluate $ReSi_n$ ($n = 1-12$) fragmentation energies and atomic averaged binding energies ($E_b(n)$), defined according to the following formula

$$E_b(n) = [nE_T(\mathrm{Si}) + E_T(\mathrm{Re}) - E_T(\mathrm{ReSi}_n)]/n$$

$$D(n, n-1) = E_T(\mathrm{ReSi}_{n-1}) + E_T(\mathrm{Si}) - E_T(\mathrm{ReSi}_n)$$

where $E_T(ReSi_{n-1})$, E_T(Si), E_T(Re), and $E_T(ReSi_n)$ are the total energies of the most stable $ReSi_{n-1}$, Si, Re, and $ReSi_n$ clusters, respectively. The total energies of the Si atom with singlet, triplet, and quintet spin configurations are −3.7193, −3.7635, and −3.6182 hartrees, respectively. The total energy of the most stable Re atom with sextet spin configuration is −78.8952 hartrees, and the theoretical results show that the Si atom with spin triplet configuration is the most stable structure. The change in total energy upon removing one Si atom from the cluster is observed, where in each case the $ReSi_n$ ($n = 1-12$) structures are compared. Our interesting findings of D(2, 1), D(3, 2), D(4, 3), D(5, 4), D(6, 5), D(7, 6), D(8, 7), D(9, 8), D(10, 9), D(11, 10), and D(12, 11) at the UB3LYP/LanL2DZ level are 3.7371, 3.4524, 3.2122, 2.8921, 3.7802, 3.6035, 3.3547, 3.9762, 2.9564, 3.8035, and 4.4078 eV, respectively. The remarkable results of D(12, 11), D(11, 10), and D(9,8) as well as D(3, 2) and D(2, 1) are found. Our results reveal that D(12, 11) is larger than D(11, 10) and D(9, 8); in other words, the $ReSi_{12}$ cluster is more stable than $ReSi_9$ and $ReSi_{11}$ clusters with respect to the removal one silicon atom. Corresponding to the lowest-energy fragmentation pathway of all $ReSi_n$ ($n = 1-12$), these findings show that $ReSi_{12}$, $ReSi_{11}$, $ReSi_9$, and $ReSi_3$ as well as $ReSi_2$ have enhanced stability and could be produced with high abundance in the mass spectrum; however, $D(n, n-1)$($n = 4$, 5, 8) are small and have low abundance in mass spectrum. Comparison of these observations with experiment measurements is made,[3] which gives firm support to our theoretical results. However, theoretical results of D(7, 6) and D(6, 5) deviate from the experimental measurement;[3] it seems that D(7, 6) and D(6, 5) are overestimated. According to our theoretical results of total energies (E_T's) for $ReSi_n$ ($n = 1-12$) clusters (Table 2), a general trend of stability is found, which is different from previous results for Ge_n ($n = 2-6$) as part of Ge_nF^- ($n = 2-6$) and Ge_nX (X = Sn, Cl) clusters[34−36] and those of MSi_n (M = Cr, Mo, W, Ag, Ir) ($n = 1-6$) clusters.[2,4,6,8,9,36] Theoretical results also indicate that $ReSi_n$ ($n = 1-6$) clusters are not characterized by the same Si_n ($n = 1-6$) framework structures as MSi_n (M = Cr, Mo, W, Cu, Ag, Ir; $n = 1-6$).[4,6,8,9,29,37]

The atomic averaged binding energy ($E_b(n)$) of the most stable $ReSi_n$ ($n = 1-12$) clusters is calculated at the B3LYP/LanL2DZ level. In light of the theoretical results summarized at Table 1, one can find that the remarkable results of E_b(2), E_b(3), E_b(9), E_b(10), E_b(11), and E_b(12) are 3.2924, 3.9713, 3.3378, 3.2998, 3.3454, and 3.4340 eV, respectively, which are bigger than those of $E_b(n)$ ($n = 4$, 7, 8), reflecting that the $ReSi_2$, $ReSi_3$, $ReSi_9$, $ReSi_{10}$, $ReSi_{11}$, and $ReSi_{12}$ clusters have enhanced stabilities which are regarded as the pronounced abundance of $ReSi_x$

($x = 2, 3, 9-12$) clusters as the observed clusters in mass spectrometric experiment.[3] Generally, this observation of relative stability obtained by $E_b(n)$ is in good agreement with that of fragmentation energy. Furthermore, $E_b(12)$ is the biggest one and the most stable one which reminds us of the so-called octet rule.[3] Unfortunately, the calculated $E_b(5)$ and $E_b(6)$ deviate from the experimental measurements.

4. Conclusions

Theoretical investigations of the $ReSi_n$ ($n = 1-12$) clusters with doublet, quartet, and sextet spin configurations are investigated at the UB3LYP level using LanL2DZ basis sets. The total energies, equilibrium geometries, and stabilities of $ReSi_n$ ($n = 1-12$) clusters, together with fragmentation energies and atomic averaged binding energies as well as natural populations and natural electron configurations, are presented and discussed. The charges in the most stable $ReSi_n$ ($n = 1-12$) clusters transfer from 6s orbitals of the Re atom and Si atoms to 5d orbitals of the Re atom. The natural populations of 5d orbitals of Re in the most stable $ReSi_n$ ($n = 1, 2$) and $ReSi_n$ ($n = 3-7$) as well as $ReSi_n$ ($n = 8-12$) clusters are about 6, 7, and 8, respectively. Theoretical results of natural populations of the most stable $ReSi_n$ ($n = 1-12$) clusters show that the natural electron configurations of 5d and 6s orbitals for the most stable $ReSi_n$ ($n = 1-12$) clusters, together with natural population of Re being recorded as negative, correlate with spin configurations and the number of coordinated silicon atoms. Re acts as an acceptor, and the charges transferred from the Si to the Re atom are bounded to 5d orbitals of the Re atom. This observation of the theoretical results gives an explanation of the efficiency of semiconductor is degraded after Re is inserted into Si bulk. The electrostatic interactions among Re and Si atoms play important roles in the stabilities of the clusters investigated. The degree of 5d shell saturation in Re influences the stability of the $ReSi_n$ ($n = 1-12$) clusters. The most stable $ReSi_n$ ($n = 2-12$) clusters correspond to the spin doublet configuration. However, the most stable ReSi is spin quartet configuration. On the basis of the equilibrium geometry analyses, it apparently indicates that the transition metal Re atom in the most stable $ReSi_n$ ($n = 1-7$) clusters absorbs on the surface site of silicon frame; however, the Re atom in the most stable $ReSi_n$ ($n = 8-12$) clusters exhibits a tendency to localize at the center site of the silicon frame. Therefore, $Re@Si_8$ turns out to be the smallest cage. This finding of Re in the most stable $ReSi_n$ ($n = 8-12$) localized at the center site of the silicon frame when $n > 7$ is in good agreement with an experimental observation of $TbSi_x^-$ ($x = 6-16$) that is available.[38] Re in $ReSi_n$ ($n = 8-12$) tries to terminate the dangling bond of the Si frame. The theoretical findings reveal why TM prefers to dope into Si bulk experimentally. Furthermore, the threshold number of silicon atom in $TMSi_n$ clusters with TM doping into Si frame varies with the type of TM atom. Growth patterns in the most stable $ReSi_n$ ($n = 9-12$) clusters are discussed showing the sandwichlike structure as the favorable geometry. The discussions on fragmentation energy and atomic averaged binding energy indicate that the lowest-energy $ReSi_n$ ($n = 2, 9, 11, 12$) clusters are more stable than the other ones, and a comparison with available experimental measurements is made. Compared to our previous theoretical results of MSi_n (M = Cr, Mo, W, Ir; $n = 1-6$), the structures identified for the most stable $ReSi_n$ isomers are actually different from MSi_n (M = Cr, Mo, W, Ir, and Cu), showing different growth patterns of these clusters.

Acknowledgment. This work is supported by National Natural Science foundation of P. R. China (20173055), National Natural Science Foundation of China (cooperation item of west and east,10247007), Natural Science Foundation of ShaanXi province (2002A09), and Special Item Foundation of Educational Committee of ShaanXi province(02JK050).

References and Notes

(1) Xiao, C.; Abraham, A.; Quinn, R.; Hagelberg, F.; Lester, W. A., Jr. *J. Phys. Chem. A* **2002**, *106*, 11380.
(2) Han, J. G.; Shi, Y. Y. *Chem. Phys.* **2001**, *266*, 33.
(3) Hiura, H.; Miyazaki, T.; Kanayama, T. *Phys. Rev. Lett.* **2001**, *86*, 1733
(4) Han, J. G.; Hageberg, F. *THEOCHEM* **2001**, *549*, 165.
(5) Xiao, C.; Hageberg, F.; Lester, W. A. *Phys. Rev. B* **2002**, *66*, 75425
(6) Han, J. G.; Xiao, C.; Hageberg, F. *Struct. Chem.* **2002**, *13*, 173.
(7) Turker, L. *THEOCHEM* **2001**, *548*, 185.
(8) Han, J. G.; Hageberg, F. *Chem. Phys.* **2001**, *263*, 255.
(9) Han, J. G. *Chem. Phys.* **2003**, *286*, 181.
(10) Han, J. G.; Ren, Z. Y.; Sheng, L. S.; Zhang, Y. W.; Morales, J. A.; Hagelberg, F. *THEOCHEM* **2003**, *625*, 47.
(11) Beck, S. B. *J. Chem. Phys.* **1989**, *90*, 6306.
(12) Scherer, J. J.; Paul, J. B.; Collier, C. P.; Saykally, R. J. *J. Chem. Phys.* **1995**, *102*, 5190.
(13) Miyazaki, T.; Hiura, H.; Kanayama, T. *Phys. Rev. B* **2002**, *66*, 121403.
(14) Yuan, Z. S.; Zhu, L. F.; Tong, X.; Liu, X. J.; Xu, K. Z. *THEOCHEM* **2002**, *589*, 229.
(15) Kumar, V.; Kawazoe, Y. *Phys. Rev. Lett.* **2002**, *88*, 235504.
(16) Ovcharenko, I. V.; Lester, W. A.; Xiao, C.; Hageberg, F. *J. Chem. Phys.* **2001**, *114*, 9029.
(17) Scherer, J. J.; Paul, J. B.; Collier, C. P.; Saykally, R. J. *J. Chem. Phys.* **1995**, *103*, 113.
(18) Turski, P. *Chem. Phys. Lett.* **1999**, *315*, 115.
(19) Harrick, Y. M.; Weltner, W., Jr. *J. Chem. Phys.* **1991**, *94*, 3371.
(20) Kingcade, J. E., Jr.; Gringerick, K. A. *J. Chem. Soc., Faraday Trans.* **1989**, *285*, 195.
(21) Gringerick, K. A. *J. Chem. Phys.* **1969**, *50*, 5426.
(22) Auwera-Mahieu, A. V.; Melntyre, N. S.; Drowert, J. *Chem. Phys. Lett.* **1969**, *4*, 198.
(23) Jackson, K.; Nellermoe, B. *Chem. Phys. Lett.* **1996**, *254*, 249.
(24) Li, F.; Ren, Z. Y.; Guo, P.; Han, J. G. To be submitted.
(25) Frisch, M. J.; Trucks, G. W.; Schlegel, H. B.; Scuseria, G. E.; Robb, M. A.; Cheeseman, J. R.; Zakrzewski, V. G.; Montgomery, J. A., Jr.; Stratmann, R. E.; Burant, J. C.; Dapprich, S.; Millam, J. M.; Daniels, A. D.; Kudin, K. N.; Strain, M. C.; Farkas, O.; Tomasi, J.; Barone, V.; Cossi, M.; Cammi, R.; Mennucci, B.; Pomelli, C.; Adamo, C.; Clifford, S.; Ochterski, J.; Petersson, G. A.; Ayala, P. Y.; Cui, Q.; Morokuma, K.; Malick, D. K.; Rabuck, A. D.; Raghavachari, K.; Foresman, J. B.; Cioslowski, J.; Ortiz, J. V.; Stefanov, B. B.; Liu, G.; Liashenko, A.; Piskorz, P.; Komaromi, I.; Gomperts, R.; Martin, R. L.; Fox, D. J.; Keith, T.; Al-Laham, M. A.; Peng, C. Y.; Nanayakkara, A.; Gonzalez, C.; Challacombe, M.; Gill, P. M. W.; Johnson, B. G.; Chen, W.; Wong, M. W.; Andres, J. L.; Head-Gordon, M.; Replogle, E. S.; Pople, J. A. *Gaussian 98*; Gaussian, Inc.: Pittsburgh, PA, 1998.
(26) Lee, C.; Yang, W.; Parr, R. G. *Phys. Rev. B* **1988**, *27*, 785.
(27) Wadt, W. R.; Hay, P. J. *J. Chem. Phys.* **1985**, *82*, 284.
(28) Becke, A. D. *Phys. Rev. A* **1988**, *38*, 3098.
(29) Xiao, C.; Hageberg, F.; Ovcharenko, I.; Lester, W. A. *THEOCHEM* **2001**, *549*, 181.
(30) Liu, B. X.; Gao, K. Y.; Zhu, H. N. *J. Vac. Sci. Technol., B* **1999**, *17*, 2277.
(31) Shvartsburg, A. A.; Liu, B.; Jarrold, M. F.; Ho, K. M. *J. Chem. Phys.* **2000**, *112*, 4517.
(32) Hageberg, F.; Xiao, C.; Lester, W. A., Jr. *Phys. Rev. B* **2003**, *67*, 35426.
(33) Chou, S. H.; Freeman, A. J.; Grogoras, S.; Gemtle, T. M.; Delly, B. *J. Chem. Phys.* **1988**, *89*, 5077.
(34) Han, J. G. *Chem. Phys. Lett.* **2000**, *324*, 143.
(35) Han, J. G.; Zhang, P. F.; Li. Q. X.; Gao, H.; Cao, G. Y.; Sheng, L. S.; Zhang, Y. W. *THEOCHEM* **2003**, *624*, 257.
(36) Han, J. G.; Ren, Z. Y.; Zhang, Y. W. *Chem. Phys.*, in press.
(37) Zhang, P. F.; Han, J. G.; Pu, Q. R. *THEOCHEM* **2003**, *635*, 25.
(38) Ohara, M.; Miyajima, K.; Pramann, A.; Nakajima, A.; Kaya, K. *J. Phys. Chem. A* **2002**, *106*, 3702.